

## Accepted Manuscript

Title: Solvent effects in hydrodeoxygenation of furfural-acetone ALDOL condensation products over Pt/TiO<sub>2</sub> catalyst

Author: Rubén Ramos Zdeněk Tišler Oleg Kikhtyanin David Kubička



PII: S0926-860X(16)30562-2  
DOI: <http://dx.doi.org/doi:10.1016/j.apcata.2016.11.023>  
Reference: APCATA 16071

To appear in: *Applied Catalysis A: General*

Received date: 26-9-2016  
Revised date: 14-11-2016  
Accepted date: 15-11-2016

Please cite this article as: Rubén Ramos, Zdeněk Tišler, Oleg Kikhtyanin, David Kubička, Solvent effects in hydrodeoxygenation of furfural-acetone ALDOL condensation products over Pt/TiO<sub>2</sub> catalyst, *Applied Catalysis A, General* <http://dx.doi.org/10.1016/j.apcata.2016.11.023>

This is a PDF file of an unedited manuscript that has been accepted for publication. As a service to our customers we are providing this early version of the manuscript. The manuscript will undergo copyediting, typesetting, and review of the resulting proof before it is published in its final form. Please note that during the production process errors may be discovered which could affect the content, and all legal disclaimers that apply to the journal pertain.

# SOLVENT EFFECTS IN HYDRODEOXYGENATION OF FURFURAL-ACETONE ALDOL CONDENSATION PRODUCTS OVER Pt/TiO<sub>2</sub> CATALYST

Rubén Ramos<sup>1,\*</sup>, Zdeněk Tišler<sup>1</sup>, Oleg Kikhtyanin<sup>1</sup>, David Kubička<sup>1,2</sup>

<sup>1</sup>*Research Institute of Inorganic Chemistry, RENTECH-UniCRE, Chempark Litvínov, Záluží-Litvínov, 436 70, Czech Republic*

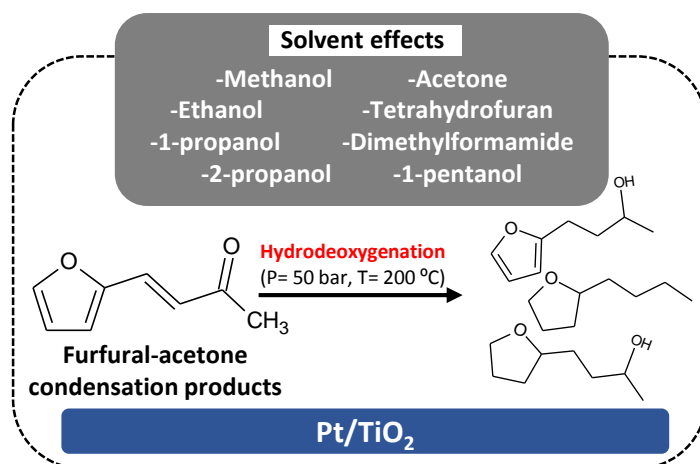
<sup>2</sup>*Technopark Kralupy, University of Chemistry and Technology Prague, Žižkova 7, 27801 Kralupy nad Vltavou, Czech Republic*

*\*Corresponding author: Ruben Ramos Velarde*

*Present address: Department of Chemistry, University of Liverpool, Crown Street, Liverpool L69 7ZD, U.K.*

*e-mail: R.Ramos-Velarde@liverpool.ac.uk*

***Graphical abstract***



### Highlights

- The hydrogenation rate and further transformations of furfural acetone condensate product are discussed considering solvent effects.
- Important differences were observed among the investigated solvents, achieving the best HDO activities when using 2-propanol and acetone.
- This work provides a better understanding of the role of a solvent, contributing to a rational selection that would improve the overall conversion efficiency.

### Abstract

The solvent effects on hydrodeoxygenation (HDO) of 4-(2-furyl)-3-buten-2-one (F-Ac) over Pt/TiO<sub>2</sub> catalyst were investigated at T=200 °C and P(H<sub>2</sub>)=50 bar. The initial reactant is the main product of aldol condensation between furfural and acetone, which constitutes a promising route for the production of bio-based chemicals and fuels. A sequence of experiments was performed using a selection of polar solvents with different chemical natures: protic (methanol, ethanol, 1-propanol, 2-propanol, 1-pentanol) and aprotic (acetone, tetrahydrofuran (THF), n,n-dimethylformamide (DMF)). In case of protic solvents, a good correlation was found between the polarity parameters and conversion. Consequently, the highest hydrogenation rate was observed when 2-propanol was used as a solvent. In contrast, the hydrogenation activity in presence of aprotic solvents was related rather to solvent-catalyst interactions. Thus, the initial hydrogenation rate declined in order

Acetone>THF>DMF, *i.e.* in accordance with the increase in the nucleophilic donor number and solvent desorption energy. Regarding the product distribution, a complex mixture of intermediates was obtained, owing to the successive hydrogenation (aliphatic C=C, furanic C=C and ketonic C=O bonds), ring opening (via C-O hydrogenolysis) and deoxygenation reactions. Based on the proposed reaction scheme for the conversion of F-Ac into octane, the influence of the studied solvents over the cascade catalytic conversion is discussed. A significant formation of cyclic saturated compounds such as 2-propyl-tetrahydropyran and 2-methyl-1,6-dioxaspiro[4,4]nonane took place via undesirable side reactions of cyclization and isomerization. The best catalytic performance was found when using acetone and 2-propanol as solvents, achieving significant yields of 4-(2-tetrahydrofuryl)-butan-2-ol (28.5-40.4 %) and linear alcohols (6.3-10.4 %). The better performance of these solvents may be associated with a lower activation energy barrier for key intermediate products, due to their moderate interaction with the reactant and the catalyst. In case of methanol and DMF, undesired reactions between the reactant and the solvent took place, leading to a lower selectivity towards the targeted hydrodeoxygenated products.

**Keywords:** Furfural, aldol condensation, hydrodeoxygenation, solvent effects, platinum titania catalyst.

## 1. Introduction

Biomass is a key renewable resource with the potential to satisfy at least partially the growing energy demand and to provide alternative technologies to petroleum-based ones. Hemicellulose is one of the major components (25-35 wt%) of non-food lignocellulose biomass, which can be transformed into C<sub>5</sub> and C<sub>6</sub> sugars monomers via acid-catalyzed hydrolysis [1,2]. This sugar fraction can be further processed to furanic compounds (via acid-catalyzed dehydration), leading to the production of lignocellulosic platform molecules (e.g. furfural and 5-hydroxymethylfurfural) that could play the role of basic building blocks in future biorefineries [3,4]. Therefore, in order to produce valuable green chemicals and fuels

from sustainable sources, the catalytic transformation of furan derivatives is regaining the attention of different research groups in recent years [5,6].

Among the different conversion strategies, aldol condensation allows increasing carbon chain length of furanic compounds by forming larger bio-based molecules, more appropriate for upgrading to gasoline and diesel fuels. Aldol condensation is a well-known organic synthesis, which generally takes place between carbonyl groups at low temperatures (25-70 °C) and atmospheric pressure. This route has been successfully used for the condensation of furfural (C<sub>5</sub>) with acetone in presence of solid basic catalysts, yielding mostly 4-(2-furyl)-3-buten-2-one (F-Ac) and 1,5-difuryl-1,4-pentadien-3-one (F-Ac-F) [7,8]. However, compared with most petrochemical products, furfural-acetone condensation products are multifunctionalized oxygenated compounds which require challenging chemical transformations *i.e.* hydrogenation (C=C aliphatic, C=O ketone and C=C furanic ring bonds), ring opening (C-O hydrogenolysis) and deoxygenation (via dehydration or C-OH hydrogenolysis) in order to yield liquid transportation fuels. Hence, the overall conversion of these adducts into alkanes may be performed by hydrodeoxygenation (HDO), generally at mild temperatures (150-300 °C) and high hydrogen pressures (20-100 bar) [9,10].

The presence of heterogeneous catalysts in the HDO processing of furfural-acetone condensation products favours the conversion rates (thermodynamic and kinetic considerations) and allows tailoring the product distribution through the selection of the catalyst features. In a previous work, we have investigated the influence of different supported Pt catalysts on the HDO of furfural-acetone condensation products [11]. Similarly, different studies from the literature have reported the performance of metal-based catalysts on this process, exploring the effects of different parameters such as; nature of the metal phase [10], catalyst morphology [12,13,14], reaction system [13,15,16] and operation conditions [9,17,18]. Most of these studies have been carried out in the liquid phase, using different kinds of solvents to dissolve the solid reactants and to dissipate the heat generated from exothermic reactions. Thus, Dumesic and co-workers investigated the hydrogenation of furfural-acetone adducts employing Pd/MgO-ZrO<sub>2</sub> as catalyst in aqueous environment [15,18]. From the same research group, another work investigated the activity of Pt/SiO<sub>2</sub>-Al<sub>2</sub>O<sub>3</sub> in dehydration of these compounds using tetrahydrofuran (THF) as solvent [16]. In the same way, Lu et al. [14,17,19] carried out a series of experiments combining different solvents such as isopropanol, ethanol, THF and cyclohexane. Similarly, Gordon et. al. [9] compared the results obtained using acetic acid and methanol as solvents in deoxygenation

reactions under mild operating conditions. Additionally, HDO of furfural-acetone condensation products has been carried out in hexane [10,12] and, also using ionic liquids [20]. Nevertheless, due to the lack of systematic experimental data, the influence of the reaction media (solvents) on the activity and selectivity in the HDO of furfural-acetone condensation products has been scarcely discussed.

According to preceding works [21-24], it is expected that solvent effects have a strong influence on hydrogenation reactions, which constitute an essential initial step in the HDO processing. A general reaction scheme for F-Ac hydrogenation is shown in Figure 1. The primary C=C aliphatic hydrogenation (4-(2-furyl)-butan-2-one; **A**) is followed by further hydrogenation steps of C=C furanic ring bonds (4-(2-tetrahydrofuryl)-butan-2-one; **B**) or C=O ketone bond (4-(2-furyl)-butan-2-ol; **C**). On the pathway to the completely hydrogenated compound (4-(2-tetrahydrofuryl)-butan-2-ol; **E**), the partial hydrogenation of the latter yields a reactive intermediate (4-(2-dihydrofuryl)-butan-2-ol; **D**), which may undergo different reactions [11].

In spite of the progress in understanding solvent effects on hydrogenation reactions, much work remains to be done to unravel the influence of solvents in multi-step catalytic transformations, such as the HDO of F-Ac towards valuable alkanes, which further comprises: ring opening reactions (on metal and possibly acid sites), dehydration/hydrogenolysis (most likely on Brønsted acid sites), as well as different side reactions. Likewise, the regular use of bifunctional catalysts in such processes may increase the complexity of solvent effects owing to the likely interactions between the metal phases and the solvent [25].

In the present contribution, we aim to investigate the solvent effects on the HDO of 4-(2-furyl)-3-buten-2-one (F-Ac) in terms of conversion rates and product distribution. Pt/TiO<sub>2</sub> was selected as a reference catalyst due to the well-known hydrodeoxygenation activity of this metal phase and the enhanced accessibility provided by the titania support. A sequence of experiments was performed using a selection of polar solvents with different chemical nature: protic (methanol, ethanol, 1-propanol, 2-propanol, 1-pentanol) and aprotic (acetone, tetrahydrofuran, n,n-dimethylformamide). The initial hydrogenation rate and further transformations through furan ring opening and deoxygenation steps, are discussed considering the solvent-reactant and the solvent-catalyst interactions. To our knowledge, such systematic investigation of solvent effects on HDO of furfural-acetone condensation products has not been described previously. Therefore, this work may provide a better understanding of

the role of a solvent in this catalytic conversion, contributing to a rational solvent selection that would improve the overall process efficiency.

## 2. Experimental

### 2.1. Chemicals

Methanol (Sigma Aldrich, >99.9 %), Ethanol (Sigma Aldrich, >99.8 %), 1-propanol (Sigma Aldrich, >99.5 %), 2-propanol (Lach-Ner, >99.7 %), 1-pentanol (Sigma Aldrich, >99 %), acetone (Sigma Aldrich, >99.5 %), tetrahydrofuran (Sigma Aldrich, >99.9 %) and *n,n*-dimethylformamide (Sigma Aldrich, >99.8 %) were used without further treatment. The TiO<sub>2</sub> support and tetraammine-platinum(II) nitrate were purchased from Eurosupport Manufacturing Czechia and Sigma Aldrich, respectively, and used as received. Hydrogen was supplied from an external reservoir (Linde, >99 %).

### 2.2. Catalyst preparation

The catalyst, Pt/TiO<sub>2</sub>, was prepared by incipient wetness impregnation using tetraammine-platinum(II) nitrate (Pt(NH<sub>3</sub>)<sub>4</sub>(NO<sub>3</sub>)<sub>2</sub>) to obtain a nominal metal loading of 2 wt% (referred to mass catalyst). The deposition of Pt was carried out by adding dropwise an aqueous solution of the precursor to the support at ambient temperature. After metal incorporation, the catalyst was dried at 120 °C overnight and calcined at 500 °C in air for 6 h (heating rate 1 °C·min<sup>-1</sup>).

### 2.3. Catalyst characterization

The properties of Pt/TiO<sub>2</sub> were analyzed by different physicochemical characterization methods. The amount of incorporated Pt was determined by X-ray Fluorescence Spectroscopy (XRF) using a Philips PW 1404 UniQuant apparatus. Textural properties were determined from N<sub>2</sub> physisorption isotherms at 77 K obtained by using a Quantachrome AUTOSORB unit. Prior to the analyses, the sample was outgassed at 250 °C for 3 h flowing N<sub>2</sub>. BET equation and BJH method were used to calculate the specific surface area and the average pore size, respectively.

Acid and base sites were evaluated by temperature programmed desorption (TPD) of ammonia and carbon dioxide, respectively, employing a Micromeritics Autochem 2950 equipment. Prior to the TPD analyses, the sample (0.1 g) was reduced in situ under 10 vol% H<sub>2</sub>/Ar (25 cm<sup>3</sup>·min<sup>-1</sup>) at 350 °C for 60 min. Then, the catalyst was outgassed in flowing

helium ( $25 \text{ cm}^3 \cdot \text{min}^{-1}$ ) with a heating ramp of  $10 \text{ }^\circ\text{C} \cdot \text{min}^{-1}$  up to  $500 \text{ }^\circ\text{C}$ . The  $\text{NH}_3$  TPD measurement was started by cooling the sample down to  $180 \text{ }^\circ\text{C}$  and saturating it with ammonia ( $25 \text{ cm}^3 \cdot \text{min}^{-1}$  of  $10 \text{ vol}\% \text{ NH}_3/\text{He}$ ) for  $30 \text{ min}$ . Subsequently, the physically adsorbed  $\text{NH}_3$  was removed by flowing He ( $25 \text{ cm}^3 \cdot \text{min}^{-1}$ ) for  $60 \text{ min}$ . Finally, TPD was performed heating the Pt/TiO<sub>2</sub> catalyst in flowing He ( $25 \text{ cm}^3 \cdot \text{min}^{-1}$ ) with a rate of  $15 \text{ }^\circ\text{C} \cdot \text{min}^{-1}$  up to  $500 \text{ }^\circ\text{C}$ , and maintaining this temperature for  $30 \text{ min}$ . The CO<sub>2</sub> TPD experiment was initiated by cooling the sample to  $50 \text{ }^\circ\text{C}$  followed by saturating it with a flow of  $10 \text{ vol}\% \text{ CO}_2/\text{He}$  ( $50 \text{ cm}^3 \cdot \text{min}^{-1}$ ) at  $50 \text{ }^\circ\text{C}$  for  $30 \text{ min}$ . Afterward, the physisorbed carbon dioxide was removed by flowing He ( $25 \text{ cm}^3 \cdot \text{min}^{-1}$ ) at  $50 \text{ }^\circ\text{C}$  for  $60 \text{ min}$ . Finally, the chemically adsorbed CO<sub>2</sub> was desorbed by heating up the sample to  $900 \text{ }^\circ\text{C}$  (heating rate of  $15 \text{ }^\circ\text{C} \cdot \text{min}^{-1}$ ) in flowing He ( $25 \text{ cm}^3 \cdot \text{min}^{-1}$ ) and maintaining this temperature for  $30 \text{ min}$ .

The metal dispersion of Pt in the Pt/TiO<sub>2</sub> catalyst was determined by CO pulse chemisorption using a Micromeritics Autochem 2950 equipment. After the reduction treatment, the sample was degassed under He flow at  $500 \text{ }^\circ\text{C}$  for  $1 \text{ h}$  and then cooled down to  $50 \text{ }^\circ\text{C}$ . Subsequently, a sequence of  $5 \text{ vol}\% \text{ CO}/\text{He}$  pulses ( $500 \text{ }\mu\text{L}$ ) was introduced in a flow of He ( $50 \text{ cm}^3 \cdot \text{min}^{-1}$ ) and passed through the sample until the areas of the successive peaks remained constant. The relation between the areas of the different chemisorbed CO pulses allowed evaluating the metal dispersion as a function of metal loading and defined adsorption stoichiometry factor (1 CO/Pt atom).

Solvent interactions with Pt/TiO<sub>2</sub> catalyst were investigated by temperature programmed desorption (TPD) of the pre-adsorbed solvent. A sample of reduced Pt/TiO<sub>2</sub> catalysts was saturated at  $50 \text{ }^\circ\text{C}$  by pulse dosing of a gaseous stream of He ( $20 \text{ cm}^3 \cdot \text{min}^{-1}$ ) bubbled through the solvent. Then, the adsorbed solvent was removed under a flow of He ( $25 \text{ cm}^3 \cdot \text{min}^{-1}$ ) by increasing the temperature from  $50$  to  $500 \text{ }^\circ\text{C}$ . Different heating rates ( $10$ ,  $15$  and  $20 \text{ }^\circ\text{C} \cdot \text{min}^{-1}$ ) were used during the TPD resulting in a variation in the temperature of the desorption peak maximum. The desorption enthalpy ( $E_d$ ) was then calculated from the slope of the linear relationship between the heating rate and the temperature of the desorption peak maximum, according to the method reported by Cvetanovic and Amenomiya [26].

#### 2.4. Catalytic experiments

The catalytic conversion of 4-(2-furyl)-3-buten-2-one (Alfa Caesar, 98%) was studied in a steel  $300 \text{ ml}$  batch reactor (Parr Instrument Co.). Temperature, pressure and stirring speed were monitored and logged through a Parr 4848B acquisition interface. Prior to the experiments, the catalyst ( $0.2 \text{ g}$ ) was reduced in situ by H<sub>2</sub> flow ( $80 \text{ cm}^3 \cdot \text{min}^{-1}$ ) at  $350 \text{ }^\circ\text{C}$  for

90 min. After cooling down, a prepared solution of 1 g of 4-(2-furyl)-3-buten-2-one (F-Ac) and 150 ml of the solvent was loaded into the reactor. Then, the system was heated up to 200 °C and pressurized with H<sub>2</sub> to 50 bar, under a slow stirring speed (100 rpm). The initial reaction time was taken when the reactor reached the desired temperature and the stirring speed was increased to 1000 rpm. The hydrogen consumed during the reaction (480 min) was replenished from an external source to maintain a constant reaction pressure. Samples of products were collected at different reaction times in order to study the progress of the reaction. The identification of the resulting compounds was done by means of GC-MS analyses using a Thermo Scientific ITQ 1100 apparatus. The quantification of the product mixtures were analyzed by an Agilent 7890A GC unit (FID detectors) equipped with a HP-5 capillary column (30 m, 0.32 ID, 0.25 μm). To this end, standard reference compound like 4-(2-furyl)-3-buten-2-one (Sigma Aldrich, >95 %) was used for calibration measurements, assuming the same GC sensitivity for the rest of C<sub>8</sub> furan/tetrahydrofuran derived compounds. F-Ac conversion at time *t* (*X<sub>t</sub>*) was calculated using Equation (1):

$$X_t = \frac{[C_{F-Ac}]_{t=0} - [C_{F-Ac}]_t}{[C_{F-Ac}]_{t=0}} \cdot 100 \quad (1)$$

where  $[C_{F-Ac}]_{t=0}$  and  $[C_{F-Ac}]_t$  are the initial molar concentration and the molar concentration at time *t* of F-Ac in solution, respectively. The yield of the specie *i* at time *t* ( $[Y_i]_t$ ) was given by Equation (2):

$$[Y_i]_t = \frac{[C_i]_t - [C_i]_{t=0}}{[C_{F-Ac}]_{t=0}} \cdot 100 \quad (2)$$

where  $[C_i]_{t=0}$  and  $[C_i]_t$  are the initial molar concentration and the molar concentration at time *t* of the specie *i*, respectively.

### 3. Results and discussion

#### 3.1. Catalyst characterization

The main physicochemical properties of Pt/TiO<sub>2</sub>, characterized by the instrumental techniques described in section 2.3, are reported in Table 1.

The final Pt content in the catalysts was determined by XRF at to be 1.8 wt%, indicating an almost complete incorporation of the metal phase on the support by the used impregnation method. The nitrogen adsorption-desorption isotherm of Pt/TiO<sub>2</sub> (Figure S1 in the Supporting

Information) exhibited a profile characteristic of mesoporous materials, with a noticeable adsorption at high relative pressures ( $P/P_0 > 0.8$ ). Based on the experimental data provided by this isotherm, BET surface area ( $95 \text{ m}^2 \cdot \text{g}^{-1}$ ) and average pore size (30.4 nm) were determined. The obtained textural properties provide an appropriate specific surface area for the dispersion of the metal phase, as well as an extensive pore size, capable of accommodating the F-Ac molecules into the mesopore system without steric limitations.

Figure 2 illustrates the temperature programmed desorption curves obtained for the desorption of  $\text{NH}_3$  (Figure 2a) and  $\text{CO}_2$  (Figure 2b). The integration of the  $\text{NH}_3$  TPD curve revealed presence of acidic sites ( $0.134 \text{ meq NH}_3 \cdot \text{g}^{-1}$ ) of weak strength (maximum desorption at  $234 \text{ }^\circ\text{C}$ ). On the contrary, the total amount of basic sites, calculated from the  $\text{CO}_2$  TPD curve, was considerably higher ( $0.416 \text{ meq CO}_2 \cdot \text{g}^{-1}$ ). This value was estimated without considering the  $\text{CO}_2$  desorbed above  $500 \text{ }^\circ\text{C}$ , since, according to some authors [27,28] and, also in agreement to the performed blank test, the TPD signal obtained at those temperatures is associated with residual carbonates not removed during the calcination or outgassing steps ( $500 \text{ }^\circ\text{C}$ ). Thus, only the chemisorbed  $\text{CO}_2$  in form of bicarbonate anions of weak basic strength ( $90\text{-}110 \text{ }^\circ\text{C}$ ) and bidentate species ( $190\text{-}220 \text{ }^\circ\text{C}$ ) of medium strength, were taken into account for the quantification of the catalyst basic properties.

Finally, Pt dispersion (15.6%) and average Pt particle size (7.2 nm) were estimated by CO pulse chemisorption measurements (Figure S2). These features may be crucial for catalyst performance, since the activation of the intermediate compounds over metal centers is strongly influenced by the dispersion degree and particle size of the metal phase [29,30].

### 3.2. Conversion and initial hydrogenation rate

Following the experimental procedure defined in the section 2.4, the effects arising from the use of different solvents in the HDO of F-Ac were evaluated in terms of the reactant conversion and the initial hydrogenation rate. Control experiments without catalysts and with non-impregnated  $\text{TiO}_2$  were performed in acetone, showing a negligible conversion ( $< 5 \%$ ) and suggesting that it is the presence of  $\text{Pt}^0$  particles which allows for  $\text{H}_2$  uptake on the surface and catalyses F-Ac hydrogenation. Likewise, catalyst particle size ( $< 30 \text{ }\mu\text{m}$ ) and vigorous stirring (1000 rpm) were chosen to avoid mass transfer limitations and internal

diffusion resistance. The first hydrogenation step usually corresponds to the fast hydrogenation of the aliphatic C=C bond, which is favoured by thermodynamic conditions and the absence of steric limitations (unlike the case of the furanic ring bonds) [12,15,16]. An overview of the conversion results obtained from the performed experiments is represented in Figure 3, where the studied polar solvents were grouped according to their chemical nature into (a) protic and (b) aprotic.

Figure 3a shows a clear difference between the conversion rates of experiments carried out in methanol and 1-pentanol, and in the rest of the studied alcohols (ethanol, 1-propanol and 2-propanol). The latter group of solvents showed higher hydrogenation rates, achieving a full conversion of F-Ac already after 180 min of reaction. However, the hydrogenation rates of F-Ac when using 1-pentanol and methanol were substantially lower, leading to an incomplete conversion even after 480 min of reaction (97 and 92.5 %, respectively). Similar behaviour was observed in Figure 3b for aprotic solvents, where in acetone and tetrahydrofuran (THF) a complete conversion was reached at 240 min, whereas, due to a considerably lower hydrogenation rate, the final conversion (480 min) in *n,n*-dimethylformamide (DMF) was around 93 %.

The factors responsible for these variations may in principle originate from different phenomena, such as: interaction of the solvent with the reactant, competitive adsorption on the catalyst surface, or reactant and hydrogen solubilities. The effects related to the solubility of the reactant can be considered negligible due to the high reaction temperature (200 °C) and the excess of solvent used (1g of F-Ac per 150 ml solvent), ensuring a complete solvation of the reactant in all performed experiments. On the other hand, although in some cases solvent effects have been attributed to different hydrogen solubility measurements [31], most of the authors agree that a clear correlation cannot be established between hydrogenation activity and hydrogen solubility [22,24,32,33]. In this respect, it is worth to note that accurate data of hydrogen solubility under the operating conditions are difficult to obtain, and a limited information is available in the literature to correlate the obtained results for the whole set of studied solvents.

Concerning the influence of the solvent-reactant interactions, Table 2 summarizes polarity parameters of each solvent and the initial hydrogenation rates exhibited in them. The dipole moment ( $\mu$ ) provides information about the structure of the molecule, whereas dielectric constant ( $\epsilon_r$ ) is a useful macroscopic measurement of the solvent polarity. The initial

hydrogenation rates were determined from the change in the molar concentration of F-Ac during the first 30 min.

The experimental results presented in Table 2 do not show any correlation between the initial hydrogenation rates and the polarity parameters when the complete series of the tested solvents is considered. For instance, the highest hydrogenation activity was observed in acetone and 2-propanol in spite of the significant differences in their dipole moment (1.66 and 2.88 D, respectively). In contrast, a satisfactory correlation was found between the solvent polarity and the initial hydrogenation rate when considering only protic solvents. In general, the initial hydrogenation rate of F-Ac decreased as the polarity of the alcohol solvents increased. Thus, the variation in the dielectric constant values ( $\epsilon_r$ ) fitted reasonably well with the estimated initial hydrogenation rates. A linear correlation was found (Figure 4) with the exception of 1-pentanol, which despite having a relatively low value of  $\epsilon_r$  (13.9), presented a low initial hydrogenation rate ( $2.44 \cdot 10^{-4} \text{ mmol} \cdot \text{g}_{\text{cat}}^{-1} \cdot \text{min}^{-1}$ ). The trend showed by most of the studied alcohols may be explained considering the hydrogen bond donors nature of protic solvents. This fact may be responsible for stronger bonding between the hydroxyl group of the alcohols and the reactant (F-Ac). Thus, as the polarity increases the solvent-reactant interaction becomes more important, improving the solvation effects and hindering the adsorption of F-Ac on the catalytic surface [24,33]. The unusually lower hydrogenation activity in 1-pentanol corresponds well with similar results obtained in hydrogenation of 1-phenyl-1,2-propanedione [22]. This behaviour may be related with the higher bulkiness of 1-pentanol, which can hinder the adsorption of the molecules, leading to a lower reaction rate [34]. Nevertheless, in this particular case probably other effects such as hydrogen solubility or adsorption strength may be involved as well.

Regarding the polar aprotic solvents, the initial hydrogenation rate pattern followed the trend: Acetone>THF>DMF, differing from the polarity correlation. Thus, no relationship between the initial hydrogenation rate and polarity parameters was found for the series of polar aprotic solvents. In particular, the highest initial hydrogenation rate was observed in acetone, which has an intermediate value of both  $\mu$  and  $\epsilon_r$ . Therefore, even though polarity parameters may play a significant role in the liquid phase hydrogenation of F-Ac, other physicochemical phenomena must be considered in order to explain the observed behaviour with polar aprotic solvents. In this respect, solvent adsorption on Pt/TiO<sub>2</sub> surface may have a strong influence on the catalytic activity. Despite the polar aprotic solvents are unable to act as hydrogen donors, they are good electron pair donor solvents. Thus, in case of working with bifunctional

catalysts, the formation of strong complexes EPD/EPA (electron pair donor/electron pair acceptor) may occur through an electron transfer between the aprotic solvent (*n*-EPD) and the metal phase (*v*-EPA) [35]. Consequently, a competitive solvent-reactant adsorption may arise, blocking partially the access of F-Ac molecules to the active sites and hindering the reaction progress. Figure 5a shows the hydrogenation rates as a function of the nucleophilic donor number (DN), which represents a quantitative measure of the electron pair donor ability [36].

The initial hydrogenation rates showed a continuous decrease as DN of the polar aprotic solvents increased. For example, the best initial hydrogenation rate exhibited in acetone corresponded with the lowest DN ( $71 \text{ kJ}\cdot\text{mol}^{-1}$ ), whereas the limited hydrogenation activity showed by DMF is related to the highest DN ( $111.2 \text{ kJ}\cdot\text{mol}^{-1}$ ). These results may also be described as a coordinative Lewis base/acid interaction between the solvent (Lewis base) and the catalyst. Consequently, considering the accepted Lewis acid character of the Pt/TiO<sub>2</sub> catalyst (Figure 2a), a series of chemisorption experiments was performed in order to confirm the strength of the solvent-catalyst interactions. Thus, following the method reported by Amenomiya et. al [26], the desorption enthalpy was calculated for each solvent and plotted as a function of the initial hydrogenation rate (Figure 5b). The maximum desorption enthalpy was found for DMF, showing a value of  $263 \text{ kJ}\cdot\text{mol}^{-1}$ . On the contrary, acetone and THF presented considerably lower desorption enthalpies of 108 and  $150 \text{ kJ}\cdot\text{mol}^{-1}$ , respectively. These results were consistent with DN data for polar aprotic solvents [36], showing a close correlation, and consequently, a very similar decreasing tendency of the initial hydrogenation rates ( $r_0$ ) as energy of desorption ( $E_d$ ) increased (Figure 5a and b). These facts suggest that DMF interacts much stronger than THF and acetone with Pt/TiO<sub>2</sub> surface, promoting a competitive solvent/reactant adsorption on the catalyst active sites. Similarly, the higher hydrogenation rate observed in acetone would be related to the weaker adsorption of this solvent on Pt/TiO<sub>2</sub>. In summary, we can conclude that solvent adsorption strength played an essential role in determining the F-Ac initial hydrogenation rate when polar aprotic solvents were used. On contrary, in the case of polar protic solvents the desorption enthalpies are not a so useful parameter due to the existence of other larger interactions like hydrogen bonding [35].

Obviously, it would have been interesting to complete the study using some apolar solvents, which are expected to show very weak interactions with both the reactant and the catalyst. However, from our own experience, 4-(2-furyl)-3-buten-2-one is nearly immiscible in both

apolar solvents and in water, limiting the F-Ac concentration in the vicinity of the accessible active sites and inducing mass transfer limitations.

### 3.3. Hydrodeoxygenation products

The experimental data allowed elucidating that the transformation of F-Ac on bifunctional catalysts started with the initial hydrogenation of aliphatic C=C bond followed by further hydrogenation steps catalyzed by metals and continued by subsequent ring opening and deoxygenation reactions on acid and metal sites, respectively. According to a previous study [37], the further hydrogenation of the carbonyl group is more demanding since it is limited by the presence of the furan ring, which causes significant steric hindrances. In this respect, the hydrogenation of the furan ring is strongly influenced by the reactant adsorption mode on the metal sites, which is closely related to the metal dispersion and metal particle size [38]. Regarding the ring-opening and deoxygenation reactions, they typically require the presence of strong acid sites that facilitate C-O hydrogenolysis and dehydrations steps [39]. Figure 6 displays an example of the evolution of the yields of the main products from the HDO of F-Ac when using acetone as a solvent. Based on the information provided by these kinetic curves, a reaction scheme was proposed in a previous work, demonstrating that a very complex mixture of products related through different catalytic transformations is formed [11].

Figure 6 clearly shows that the first hydrogenation step of C=C aliphatic bond, forming 4-(2-furyl)-butan-2-one (**A**), is followed by formation of further hydrogenated products such as: 4-(2-tetrahydrofuryl)-butan-2-one (**B**), 4-(2-furyl)-butan-2-ol (**C**) and 4-(2-dihydrofuryl)-butan-2-ol (**D**). The presence of a maximum in the yield of those compounds reveals their intermediate character on the pathway towards the fully hydrogenated molecule 4-(2-tetrahydrofuryl)-butan-2-ol (**E**), which shows a continuous increase as the reaction proceeds. A similar trend is observed in the case of 2-butyl-dihydrofuran (**G**) and 2-butyl-tetrahydrofuran (**H**), which are formed most probably by dehydration steps and subsequent ring hydrogenation of the primary products. The continuously increasing yield of these compounds (**E**, **G** and **H**) indicates a limitation in the subsequent ring opening steps on the conversion pathway of F-Ac to linear alcohols over Pt/TiO<sub>2</sub> catalyst. This fact is likely associated with the absence of stronger acid sites (mainly Brønsted), which, in combination with metal sites, are mostly responsible for ring-opening reactions typically through C-O hydrogenolysis. Nevertheless, in case of acetone as a solvent, a significant formation of

octanediols and octanols (**J**) took place ( $\approx 10\%$ ), suggesting that ring opening takes place though to a limited extent.

The use of Pt/TiO<sub>2</sub> as a catalyst for the study of the solvent effects is justified by its multifunctional properties (metal sites and weak acidity/basicity) as well as by the absence of stronger basic/acid sites, which usually, under the selected operation conditions, promote side reactions with the solvent [11,40]. This selection was based on our previous work [11], in which Pt/TiO<sub>2</sub> catalyst showed the best conversion rate of furfural-acetone adducts and the lowest formation of solvent-reactants condensates. Thus, the use of weakly basic/acid support can be a suitable strategy to modify the catalyst performance, as long as the basicity/acidity is not strong enough to catalyze undesired reaction steps like aldol condensation, etherification or acetalization.

The above presented differences in F-Ac conversion rates could be also applied when discussing the concentration of intermediate compounds derived from the tandem reaction pathway of the studied HDO conversion [11,12]. Thus, solvent-reactant and solvent-catalyst interactions may affect the kinetics of each step, leading to major changes as the reaction proceeds. Figure 7a shows the yields of the main hydrogenated products at the end of the reaction time (480 min). Thereby, important differences in the product distribution may be appreciated between the tested solvents. For example, the yield of **A** varies from 0 % in case of 2-propanol to 60.5 % for methanol. Similar deviations can be found in the production of **B**, **C** and **E** showing their maximum yields in ethanol (16 %), THF (47.8 %) and 2-propanol (40.4 %), respectively. However, these variations may be considerably reduced if we refer to the results in terms of selectivity. Since the reaction time needed to reach full conversion of the initial reactant (F-Ac) is very different in each experiment depending on the solvent used, the yields of the hydrogenated products showed in Figure 7a could be strongly influenced by the conversion degree of F-Ac. In this respect, Figure 7b represents the product distribution obtained with each solvent when considering the same conversion degree of F-Ac (i.e. 70 %). Thus, for instance, the yield of **A** varies within a much narrower range (50-61 %). Likewise, the yield variations of **B**, **C**, **D** and **E** are substantially reduced when the conversion of F-Ac is the same for each solvent. Hence, the results presented in Figure 7 suggest that the yields of the products are strongly dependent on the conversion rates showed by each solvent, having a deeper impact due to the cascade reaction of the studied HDO conversion.

Table 3 summarizes the final yields (after 480 min) of the products from HDO of F-Ac in experiments using different solvents. As discussed above, it is important to mention that these results are primarily affected by the different hydrogenation rates showed by each solvent. The results derived from the use of DMF were not included in this table owing to the totally different product distribution obtained in this solvent media. This behaviour will be discussed in detail separately hereafter.

The catalytic performance of Pt/TiO<sub>2</sub> varied significantly depending on the applied solvent. In case of methanol, the reaction practically seized after the primary hydrogenation (**A**=60.5 %) and did not proceed further. As it has been previously reported [23,41], the smaller and more reactive is the alcohol the stronger is the hydrogen bonding between the carbonyl oxygen of the reactant and the hydroxy group of the solvent. Thus, in case of methanol the interaction was the most pronounced among the used solvents, reducing thus the preference towards C=O hydrogenation intermediate (**C**), which constitutes the preferred pathway in the following hydrogenation steps. The hydrogenation of the C=C furanic bonds (yielding **B**) is relatively limited in F-Ac due to the aromatic nature of the furan ring and also owing to the presence of the C=O bond in the same adsorption plane [42]. Thus, a selective hydrogenation of the C=O bond (**C**) took usually preference over the hydrogenation of furanic C=C (**B**) in most of the performed experiments. On the other hand, a significant yield (19.3 %) of heavier products (molecular mass over 146 g·mol<sup>-1</sup>) were found in case of using methanol. This fact is in agreement with previous works reporting that shorter chain alcohols favour side reactions like acetalization [33] or etherification [41,43] between the reactant and the solvent. The formed acetal and ether intermediates may undergo further conversions at longer reaction times and/or higher temperatures, producing equally interesting hydrodeoxygenated by-products [44,45].

Similarly to methanol, the experiment carried out with 1-pentanol showed a high selectivity to the primary hydrogenated product (**A**=57 %), although in this case a significant hydrogenation of the C=O bond (**C**=28 %) was also observed. This fact can be attributed to the less effective hydrogen bonding between the solvent OH group and the reactant, due to the larger molecular size of 1-pentanol. In any case, according to these results, both protic solvents showed a limited HDO activity due to different causes namely strong reactant-alcohol interaction (methanol) and higher bulkiness (1-pentanol) which retarded F-Ac adsorption on the catalyst [34,41].

The hydrogenation degree of F-Ac was gradually enhanced when using ethanol, 1-propanol and 2-propanol, reaching yields of **E** equal to 7.1, 15.2 and 40.4 % after 480 min, respectively. The better performance of 2-propanol over the rest of alcohols agrees well with the higher hydrogenation activity observed when secondary alcohols are used as solvents instead of primary alcohols [24,46]. This improvement in the hydrogenation ability has been attributed to an additional reduction mechanism involving H<sub>2</sub> transfer from the alcohol hydroxy group on the metal surface [24] or to the more effective hydrogen donor via interhydride transfer on Lewis acid catalysts [47,48]. The noticeable production of **B** in ethanol (16 %) is probably related to the mentioned stronger hydrogen bonding (between the ketone group of the reactant and the solvent OH group) as the alcohol molecular size is reduced, preventing thereby the formation of further hydrodeoxygenated intermediates. Likewise, an important yield of 2-methyl-1,6-dioxaspiro[4,4]nonane (**F**) was observed, especially with 1-propanol (19.6 %). The formation of this compound occurs via cyclization of **D** due to the interaction between the OH group and the partially hydrogenated furanic ring [49]. Dehydration also took place resulting in the elimination of hydroxyl groups from **C**, **D** and **E**, and consequently yielding products such as: 2-butyl-dihydrofuran (**G**), and 2-butyl-tetrahydrofuran (**H**) and 2-propyl-tetrahydropyran (**I**). Similarly to the production of **F**, the formation of **I** is associated with fast hydrogenation and isomerization of the partially hydrogenated furanic ring (**G**) [50]. The concentration of **I** was quite significant in 1-propanol (17.3 %) and 2-propanol (31.7 %), suggesting a pronounced extent of isomerization/cyclization steps when using these solvents. Nevertheless, both **F** and **I** constitute an important fraction of cyclic saturated products formed by undesirable side reactions that are difficult to transform into linear hydrocarbons due to the limited ring opening activity of the Pt/TiO<sub>2</sub> catalyst.

In case of aprotic solvents, pronounced differences were found between the product distribution showed by acetone and THF. In case of THF, along with aliphatic bond hydrogenation (**A**=23 %), a prominent yield of **C** was observed (47.8 %). Equally, in spite of the low production of partially deoxygenated products (**G** and **H**), a remarkable formation of **I** was obtained (13.3 %). This fact is likely a consequence of fast isomerization/cyclization reactions when using THF as a solvent. On the other hand, the HDO of F-Ac in acetone presents the highest production of both linear alcohols (**J**=10.3 %) and partially deoxygenated products (**G**+**H**+**I**=36.2 %). It also needs to be mentioned that a significant extent of acetone self-condensation was observed, yielding mesityl oxide (0.01 g·cm<sup>-3</sup>) and methyl isobutyl

ketone ( $0.03 \text{ g}\cdot\text{cm}^{-3}$ ). Moreover, partial hydrogenation of acetone took place ( $<5\%$ ) forming 2-propanol in the reaction media. Both acetone and 2-propanol showed the highest yield of products found at the end of the HDO cascade reaction network (**J**, **G**, **H**, **I**), which is in agreement with the higher conversion rates observed with these solvents. Therefore, the better performance of these solvents may be associated with a lower activation energy barrier for the key intermediate products, leading to enhanced reactions rates. Nevertheless, unlike in 2-propanol in which only octanediols were present, the use of acetone favoured the production of **G** and **H** (15.3 %) which are the direct precursors for the formation of octanol. Its concentration in the final product mixture was 3.2 %.

The product distribution observed when using DMF differed completely from the rest of the tested solvents, showing a high selectivity ( $>80\%$ ) to the formation of two isomers of 4-(2-furyl)-3-buten-2-dimethylamine. These compounds were likely formed via thermal decomposition of DMF into carbon dioxide and dimethylamine (Figure 8a) [51], followed by the subsequent ketone amine addition between F-Ac and dimethylamine (Figure 8b). This reaction involves the formation of the corresponding hemiaminal and enamine intermediates which are rapidly converted by dehydration and hydrogenation steps, respectively. Thus, despite the high conversion of F-Ac achieved with DMF (93 %), the negligible yield of the targeted hydrodeoxygenated products discourages the use of this solvent. This fact illustrates the importance of a proper solvent selection not only with respect to conversion rates but also in terms of suppressing undesirable side reactions.

### *Conclusions*

Solvents influence the catalytic hydrodeoxygenation of 4-(2-furyl)-3-buten-2-one (F-Ac) by altering solvent-reactant and solvent-catalyst interactions. The use of Pt/TiO<sub>2</sub> as a catalyst allowed an almost complete conversion of F-Ac ( $>92\%$ ) with all the tested solvents after 480 min under  $P(\text{H}_2)=50$  bar and at  $T=200$  °C. The solvent polarity of protic solvents correlated well with the observed hydrogenation activity, indicating the importance of solvent-reactant interactions. Specifically, F-Ac conversion increased with decreasing protic solvent polarity. On the other hand, a strong interaction between the catalysts and the solvents could inhibit hydrogenation rate in case of aprotic polar solvents.

The differences in conversion rates have a strong influence on the obtained product distribution due to the complex network of reactions involved in the studied transformation.

Thus, important differences were observed among the investigated solvents, achieving the best HDO activities when using 2-propanol and acetone. Despite the formation of stable cyclic intermediates such as 2-methyl-1,6-dioxaspiro[4,4]nonane (**F**) and 2-propyl-tetrahydropyran (**I**), the use of these solvents led to a significant production of 4-(2-tetrahydrofuryl)-butan-2-ol (28.5-40.4 %) and linear alcohols (6.3-10.4 %). The production of the latter demonstrated that, besides hydrogenation reactions, ring opening took place when using acetone and 2-propanol as solvents. Likewise, undesirable condensation reactions between the solvent and the reactant were also observed with methanol (etherification) and DMF (ketone-amine addition). The results indicate that in addition to the development and design of the catalysts, the appropriate selection of the solvent media is essential in order to optimise the HDO of furan derivatives compounds.

### *Acknowledgments*

This publication is a result of the project no. P106/12/G015 supported by the Czech Science Foundation which is being carried out in the UniCRE center (CZ.1.05/2.1.00/03.0071) whose infrastructure was supported by the European Regional Development Fund and the state budget of the Czech Republic.

**References**

- [1] R.W. Torget, J.S. Kim, Y.Y. Lee, *Ind. Eng. Chem. Res.* 39 (2000) 2817-2825.
- [2] K. Karimi, S. Kheradmandinia, M.J. Taherzadeh, *Biomass Bioenergy* 30 (2006) 247-253.
- [3] Y. Román-Leshkov, J.N. Chheda, J.A. Dumesic, *Science* 312 (2006) 1933-1937.
- [4] J.J. Bozell, G.R. Petersen, *Green Chemistry* 12 (2010) 539-554.
- [5] A.S. Dias, S. Lima, M. Pillinger, A.A. Valente, *Advances in Synthetic Chemistry* 8 (2010) 167-186.
- [6] K.J. Zeitsch, *The chemistry and technology of furfural and its many by-products*. Vol. 13. Elsevier, 2000.
- [7] G.W. Huber, J.N. Chheda, C.J. Barrett, J.A. Dumesic, J. A., *Science* 308 (2005) 1446-1450.
- [8] L. Hora, V. Kelbichová, O. Kikhtyanin, O. Bortnovskiy, D. Kubička, *Catal. Today* 223 (2014) 138-147.
- [9] A.D. Sutton, F.D., Waldie, R. Wu, M. Schlaf, A. Louis III, J.C. Gordon, *Nat. Chem.* 5 (2013) 428-432.
- [10] L. Faba, E. Díaz, S. Ordóñez, *Appl. Catal. B: Env.* 160 (2014) 436-444.
- [11] R. Ramos, Z. Tišler, O. Kikhtyanin, D. Kubička, *Catal, Sci. Tech.* 6 (2016), 1829-1841.
- [12] L. Faba, E. Díaz, S. Ordóñez, *Catal, Sci. Tech.* 5 (2015) 1473-1484.
- [13] L. Faba, E. Díaz, S. Ordóñez, *Chem. Sus. Chem.* 7 (2014) 2816-2820.
- [14] Q.N. Xia, Q. Cuan, X.H. Liu, X.Q. Gong, G.Z. Lu, Y.Q. Wang, *Ang. Chem. Int. Ed.* 53 (2014) 9755-9760.
- [15] C.J. Barrett, J.N. Chheda, G.W. Huber, J.A. Dumesic, *Appl. Catal B: Env* 66 (2006) 111-118.
- [16] R. Xing, A.V. Subrahmanyam, H. Olcay, W. Qi, G.P. van Walsum, H. Pendse, G.W. Huber, *Green Chem.*, 12 (2010), 1933-1946.
- [17] W. Xu, Q. Xia, Y. Zhang, Y. Guo, Y. Wang, G. Lu, *Chem. Sus. Chem.* 4 (2011) 1758-1761.
- [18] J.N. Chheda, J.A. Dumesic, *Catal. Today* 123 (2007) 59-70.
- [19] W. Xu, X. Liu, J. Ren, P. Zhang, Y. Wang, Y. Guo, G. Lu, *Catal. Comm.* 11 (2010) 721-726.
- [20] K.L. Luska, J. Julis, E. Stavitski, D.N. Zakharov, A. Adams, W. Leitner, *Chem. Sci.* 5 (2014) 4895-4905.
- [21] P. Mäki-Arvela, L.P. Tiainen, A.K. Neyestanaki, R. Sjöholm, T.K. Rantakylä, E. Laine, T. Salmi, D.Y. Murzin, *Appl. Catal. A: Gen.* 237 (2002) 181-200.
- [22] E. Toukoniitty, P. Mäki-Arvela, J. Kuusisto, V. Nieminen, J. Päiväranta, M. Hotokka, T. Salmi, D. Murzin, *J. Mol. Cat. A: Chem.* 192 (2003) 135-151.
- [23] J. Hájek, N. Kumar, P. Mäki-Arvela, T. Salmi, D.Y. Murzin, *J. Mol. Cat. A: Chem.* 217 (2004) 145-154.

- [24] N.M. Bertero, A.F. Trasarti, C.R. Apesteguía, A.J. Marchi, *Appl. Catal. A: Gen.* 394 (2011) 228-238.
- [25] P. Mäki-Arvela, J. Hajek, T. Salmi, D.Y. Murzin, *Appl. Catal. A: Gen.* 292 (2005) 1-49.
- [26] R.J. Cvetanovic, Y. Amenomiya, *Advan. Catal. Relat. Subj.* 17 (1967) 103-149.
- [27] M. Di Serio, M. Ledda, M. Cozzolino, G. Minutillo, R. Tesser, E. Santacesaria, *Ind. Eng. Chem. Res.* 45 (2006) 3009-3014.
- [28] M. Bolognini, F. Cavani, D. Scagliarini, C. Flego, C. Perego, M. Saba, *Catal. Today*, 75 (2002) 103-111.
- [29] B. Coq, A. Tijani, F. Figuéras, *F. J. Mol. Catal.*, 68 (1991) 331-345.
- [30] A. Giroir-Fendler, D. Richard, P. Gallezot, *Catal. Lett.*, 5 (1990) 175-181.
- [31] P.A. Rautanen, J.R. Aittamaa, A.O.I. Krause, *Ind. Eng. Chem. Res.* 39 (2000) 4032-4039.
- [32] A. Drelinkiewicz, A. Waksmundzka, W. Makowski, J.W. Sobczak, A. Król, A. Zieba, *Catal. Lett.* 94 (2004) 143-156.
- [33] J. He, C. Zhao, J.A. Lercher, *J. Catal.* 309 (2014) 362-375.
- [34] I. Kun, G. Szöllösi, M. Bartók, *J. Mol. Catal. A: Chem.* 169 (2001) 235-246.
- [35] C. Reichardt, *Solvent effects in organic chemistry.* Verlag Chemie (1979).
- [36] V. Gutmann, *Electrochim. Acta* 21 (1976) 661-670.
- [37] H. Wan, A. Vitter, R.V. Chaudhari, B. Subramaniam, *J. Catal.* 309 (2014) 174-184.
- [38] W. Zang, G. Li, L. Wang, X. Zhang, *Catal. Sci. Tech.* 5 (2015) 2532-2553.
- [39] C.R. Waidmann, A.W. Pierpont, E.R. Batista, J.C. Gordon, R.L. Martin, R.M. West, R. Wu, *Catal. Sci. Tech.*, 3 (2013) 106-115.
- [40] P. Panagiotopoulou, D.G. Vlachos, *Appl. Catal. A: Gen.* 480 (2014) 17-24.
- [41] P. Panagiotopoulou, N. Martin, D.G. Vlachos, *J. Mol. Catal. A: Chem.* 392 (2014) 223-228.
- [42] R. Rao, A. Dandekar, R.T.K. Baker, M.A. Vannice, *J. Catal.* 171 (1997) 406-419.
- [43] X. Hu, R.J. Westerhof, L. Wu, D. Dong, C.Z. Li, *Green Chem.* 17 (2015) 219-224.
- [44] J. Luo, M. Monai, H. Yun, L. Arroyo-Ramírez, C. Wang, C.B. Murray, P. Fornasiero, R.J. Gorte, *Catal. Lett.*, 146 (2016) 711-717.
- [45] J. Luo, L. Arroyo-Ramírez, R.J. Gorte, D. Tzoulaki, D.G. Vlachos. *AIChE Journal*, 61 (2015) 590-597.
- [46] J.I. Di Cosimo, A. Acosta, C.R. Apesteguía, *J. Mol. Catal. A: Chem.* 234 (2005) 111-120.
- [47] M.A. Aramendía, V. Borau, C. Jiménez, J.M. Marinas, J.R. Ruiz, F.J. Urbano, *J. Mol. Catal. A: Chem.* 171 (2001) 153-158.
- [48] A. Martin, U. Armbruster, I. Gandarias, P.L. Arias, *Eur. J. Lipid Sci. Tech.* 115 (2013) 9-27.
- [49] K. Alexander, L.S. Hafner, L.E. Schniepp, *J. Am. Chem. Soc.* 73 (1951) 2725-2726.
- [50] A.A. Anderson, S.P. Simonyan, E. Lukevics, *Chem. Het. Comp.* 34 (1998) 1406-1408.

[51] J. Muzart, *Tetrahedron*, 65 (2009) 8313-8323.

## Figure captions

### Figure 1

Reaction scheme for the hydrogenation of 4-(2-furyl)-3-buten-2-one over bifunctional catalysts; **(A)** 4-(2-furyl)-butan-2-one, **(B)** 4-(2-tetrahydrofuryl)-butan-2-one, **(C)** 4-(2-furyl)-butan-2-ol, **(D)** 4-(2-dihydrofuryl)-butan-2-ol, **(E)** 4-(2-tetrahydrofuryl)-butan-2-ol.

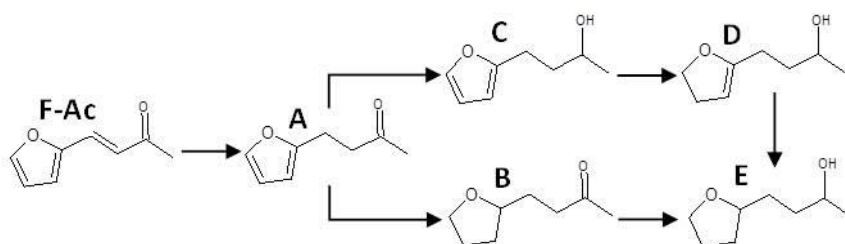


### Figure 2

TPD curves of Pt/TiO<sub>2</sub> catalyst; (a) ammonia TPD and (b) carbon dioxide TPD.

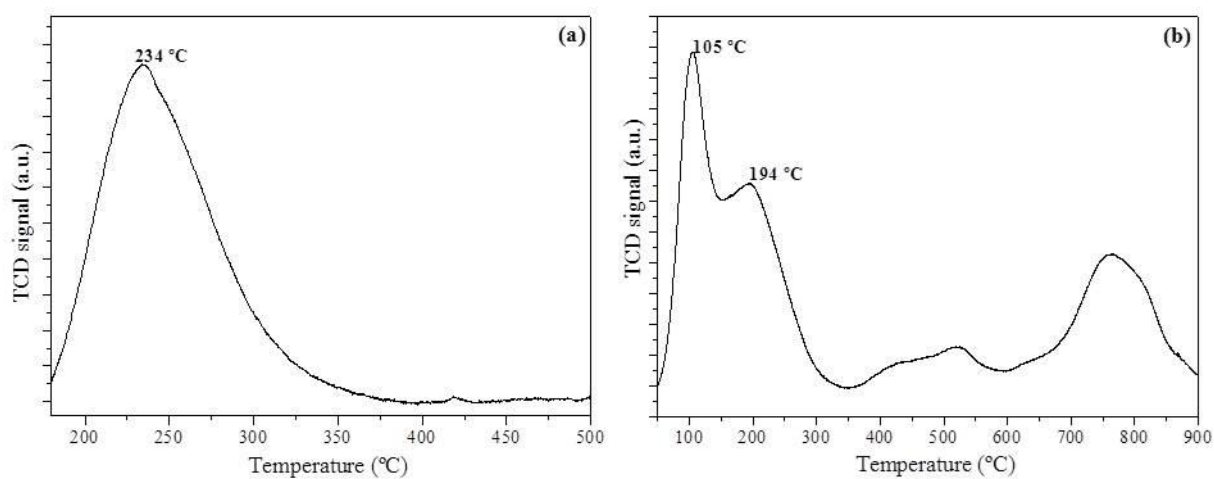


### Figure 3

Solvent effects on the conversion of 4-(2-furyl)-3-buten-2-one over Pt/TiO<sub>2</sub> catalyst; (a) protic and (b) aprotic solvents.

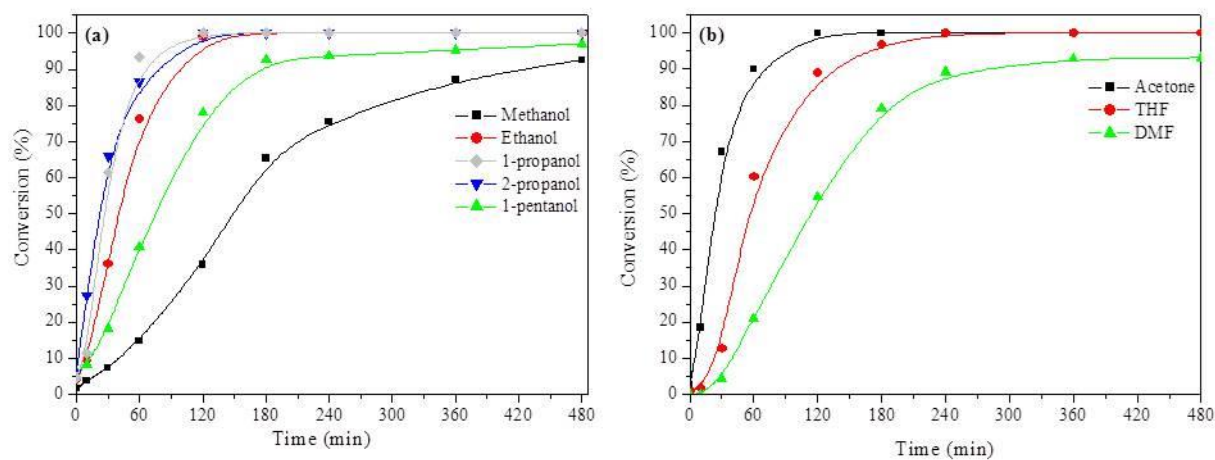
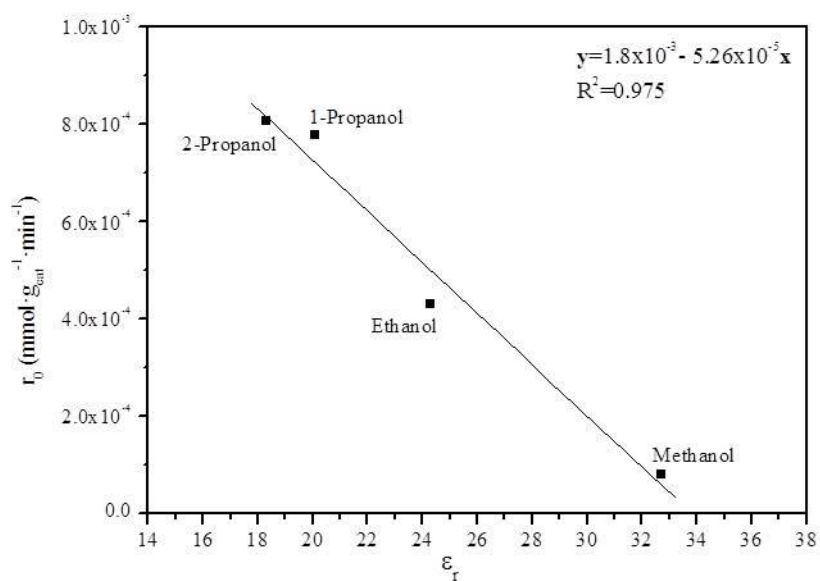


**Figure 4**

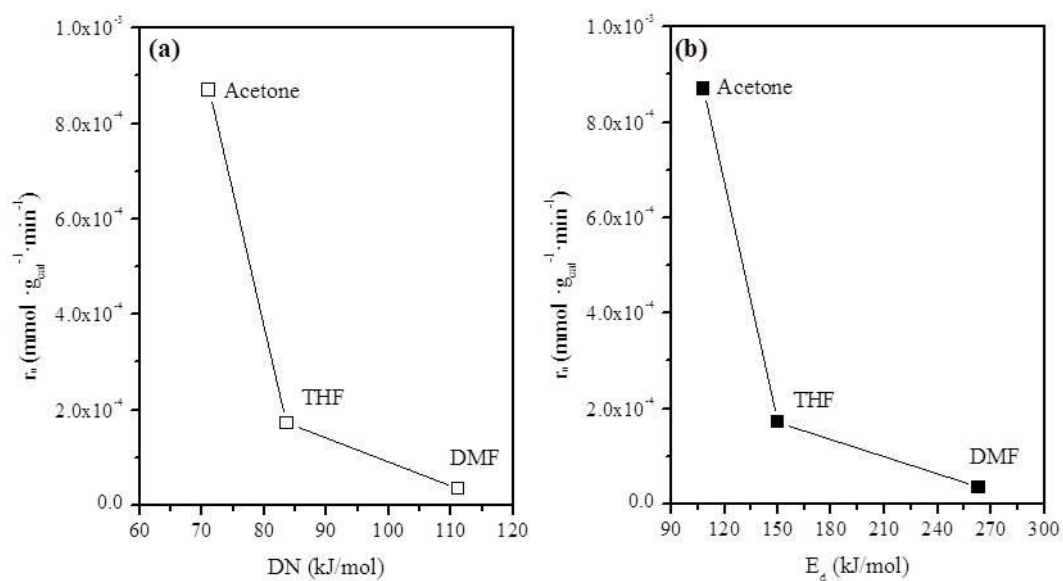
Initial hydrogenation rates as a function of solvent dielectric constants of polar protic



solvents.

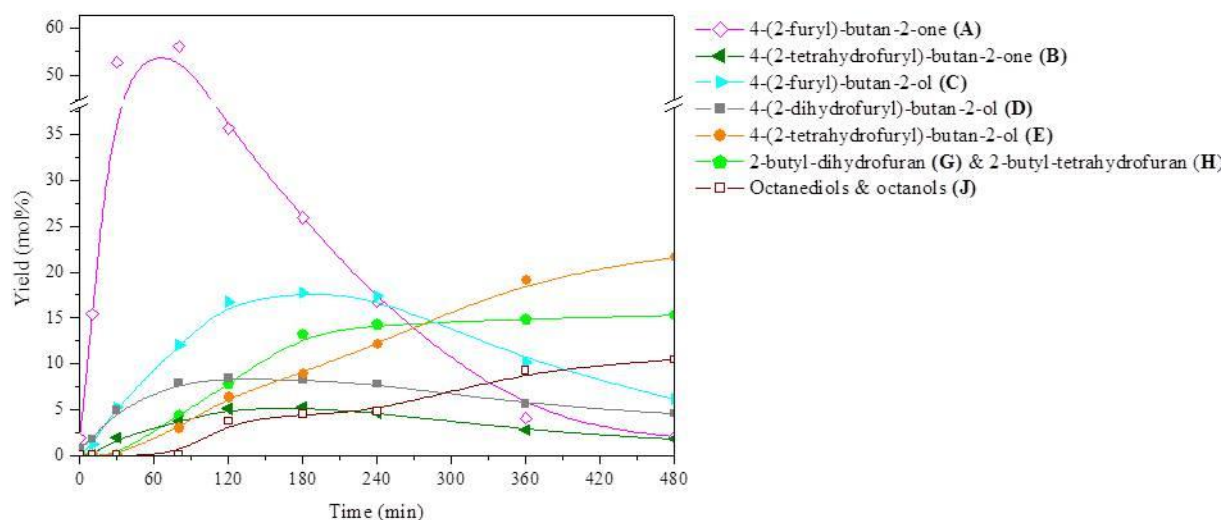
**Figure 5**

Initial hydrogenation rate of F-Ac in aprotic solvents as a function of: (a) nucleophilic donor number [36] and (b) solvent desorption energy (calculated by TPD).



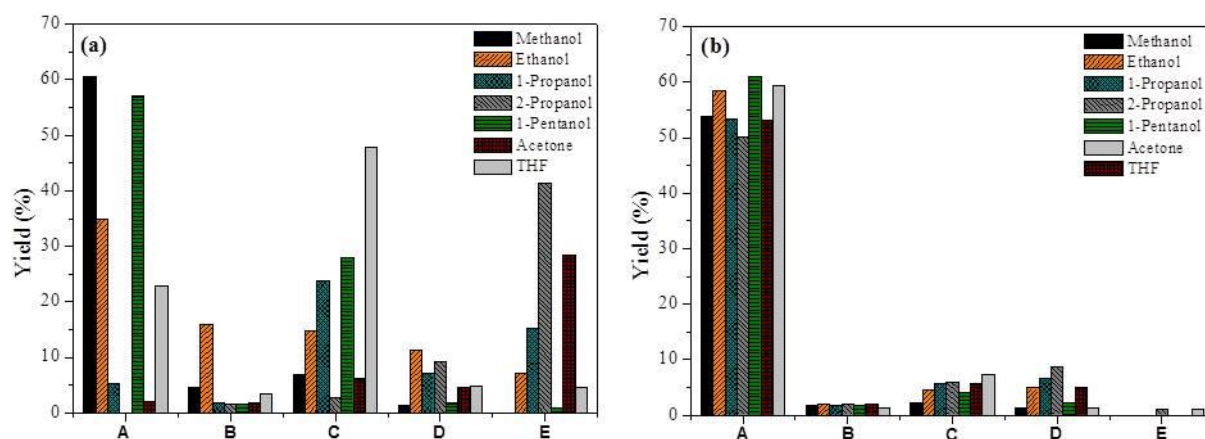
**Figure 6**

Evolution of the yields of the main products from the HDO of 4-(2-furyl)-3-buten-2-one over Pt/TiO<sub>2</sub> using acetone as solvent.



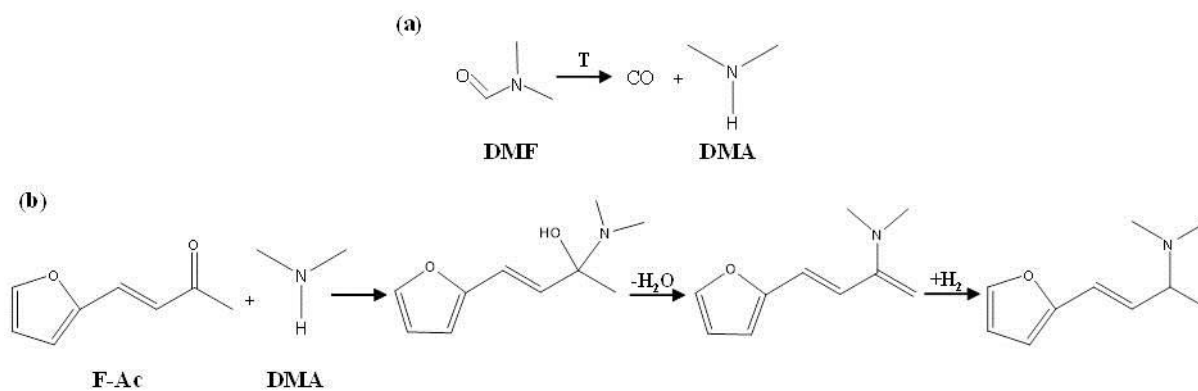
**Figure 7**

Yields of the hydrogenated products from HDO of F-Ac at (a) the end of the reaction (480 min) and (b) considering the same conversion degree of F-Ac (70 %).



**Figure 8**

Reaction scheme for (a) thermal decomposition of n,n-dimethylformamide and (b) addition of 4-(2-furyl)-3-buten-2-one and dimethylamine.

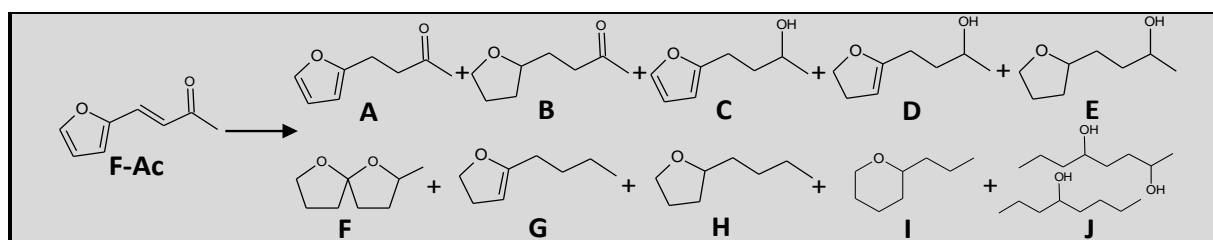


**Table 1.** Physicochemical properties of Pt/TiO<sub>2</sub> catalyst.

Pt content	(wt%)	1.8
BET surface	(m <sup>2</sup> ·g <sup>-1</sup> )	95
Pore size	(nm)	30.4
Amount of acid sites	(meq NH <sub>3</sub> ·g <sup>-1</sup> )	0.134
NH <sub>3</sub> desorption maximum	(°C)	234
Amount of base sites	(meq CO <sub>2</sub> ·g <sup>-1</sup> )	0.416
CO <sub>2</sub> desorption maximum	(°C)	105/194
Pt dispersion	(%)	15.6
Average Pt particle size	(nm)	7.2

**Table 2.** Solvent polarity parameters of the studied solvents (Dipole moment ( $\mu$ ), dielectric constant ( $\epsilon_r$ )) and initial hydrogenation rates of HDO conversion of F-Ac over Pt/TiO<sub>2</sub>.

Solvent	$\mu$	$\epsilon_r$	$r_0 \times 10^{-4}$
	Debye	(at 25 °C)	(mmol·g <sub>cat</sub> <sup>-1</sup> ·min <sup>-1</sup> )
Methanol	1.70	32.7	0.80
Ethanol	1.69	24.3	4.31
1-propanol	1.68	20.1	7.77
2-propanol	1.66	18.3	8.08
1-pentanol	1.70	13.9	2.44
THF	1.63	7.6	1.72
Acetone	2.88	20.5	8.70
DMF	3.86	36.7	0.35

**Table 3.** Yields of F-Ac hydrodeoxygenation products after 480 min (T=200 °C; P(H<sub>2</sub>)=50 bar).


Solvent	Conv. (mol%)	Yield (mol%)								
		A	B	C	D	E	F	G+H	I	J
Methanol	92.5	60.5	4.5	6.8	1.4	0	0	0	0	0
Ethanol	100	34.8	16	14.8	11.3	7.1	7.2	6.5	0	2
1-Propanol	100	5.2	1.8	23.8	7.2	15.2	19.6	9.7	17.3	0
<b>2-Propanol</b>	<b>100</b>	<b>0</b>	<b>1.6</b>	<b>2.6</b>	<b>9</b>	<b>40.4</b>	<b>8.2</b>	<b>0</b>	<b>31.7</b>	<b>6.3</b>
1-Pentanol	92	57	1.6	28	1.7	1	2.5	0	0	0
THF	100	22.9	3.4	47.8	4.7	4.6	3.1	0	13.3	0
<b>Acetone</b>	<b>100</b>	<b>2</b>	<b>1.7</b>	<b>6.1</b>	<b>4.5</b>	<b>28.5</b>	<b>10.3</b>	<b>15.3</b>	<b>20.9</b>	<b>10.4</b>